

Resource-Efficient Cooperative Online Scalar Field Mapping via Distributed Sparse Gaussian Process Regression

Tianyi Ding, Ronghao Zheng[†], Senlin Zhang, Meiqin Liu

Abstract— Cooperative online scalar field mapping is an important task for multi-robot systems. Gaussian process regression is widely used to construct a map that represents spatial information with confidence intervals. However, it is difficult to handle cooperative online mapping tasks because of its high computation and communication costs. This letter proposes a resource-efficient cooperative online field mapping method via distributed sparse Gaussian process regression. A novel distributed online Gaussian process evaluation method is developed such that robots can cooperatively evaluate and find observations of sufficient global utility to reduce computation. The error bounds of distributed aggregation results are guaranteed theoretically, and the performances of the proposed algorithms are validated by real online light field mapping experiments.

I. INTRODUCTION

Cooperative online mapping in unknown environments is a critical mission for multi-robot systems on large-scale environmental monitoring and exploration applications [1], [2], [3]. In this mission, each robot moves and measures data locally in unknown fields and then shares information with neighbors to construct the global scalar field map. The main challenge for cooperative large-scale online mapping is that large amounts of data need to be sampled, stored, and computed collaboratively in real time but local resources on each robot are limited [4], [5].

Gaussian process regression (GPR) is a framework for nonlinear non-parametric Bayesian inference widely used in field mapping [6], [7], [8]. Unfortunately, the standard GPR requires $\mathcal{O}(N^3)$ time complexity with the training sample size N , which is not suitable for large-scale online mapping due to the high cost in computation, communication, and memory. In this letter, we consider cooperative online scalar field mapping for distributed multi-robot systems and propose a resource-efficient distributed sparse Gaussian process regression method to solve these challenges.

A. Related Work

To speed up GPR, sparse variational GPR (SVGPR) is developed [9], [10], which employs a set of $M \ll N$

The authors Tianyi Ding, Ronghao Zheng, and Senlin Zhang are with the College of Electrical Engineering, Zhejiang University, Hangzhou, China. Emails: {ty_ding, rzheng, slzhang}@zju.edu.cn

The author Meiqin Liu is with the Institute of Artificial Intelligence and Robotics, Xi'an Jiaotong University, Xi'an, China. Email: liumeiqin@xjtu.edu.cn

All authors are also with the National Key Laboratory of Industrial Control Technology, Zhejiang University, Hangzhou 310027, China

[†]Corresponding author

This work was supported by the National Natural Science Foundation of China under Grant 62173294 and the NSFC-Zhejiang Joint Fund for the Integration of Industrialization and Informatization under Grant U1909206.

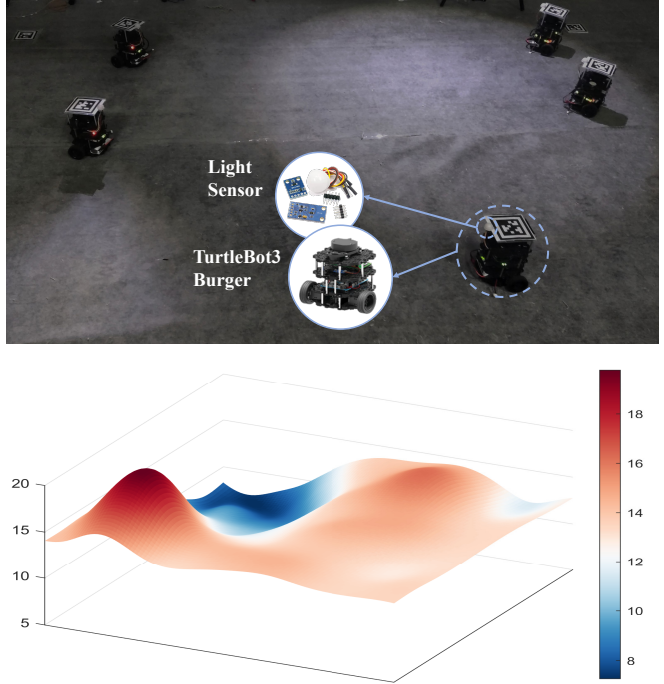


Fig. 1: Light field mapping experiments (top) and distributed light field mapping results (bottom). The value is the light intensity (lx).

pseudo-points based on KL divergence to summarize the N sample data thereby reducing computational costs to $\mathcal{O}(NM^2)$. Meanwhile, many Gaussian process aggregation methods are proposed for parallel computation, like product-of-experts (PoE) [11] and robust Bayesian committee machine [12]. Then, SVGPR combined parallel computation [13] and stochastic optimization [14] methods are developed to further reduce computational costs. Moreover, Refs. [15] and [16] provide recursive frameworks for standard GPR and sparse variational GPR to handle online streaming data. Ref. [17] combine these sparse variational, mini-batches and streaming methods and apply them to Bayesian robot model learning and control. However, these methods are centralized, in which SVGPR requires global information of the observations for sparse approximations, and the parallel methods require a central node for model aggregations. Therefore, these methods cannot be easily extended to distributed multi-robot systems since all observations and models are required to communicate across networks, which increases inter-robot communications and causes repeated computations about the same observations on different robots.

For dynamic networks without a center, distributed Gaussian process aggregation methods based on average consensus are proposed in [18], [19] and [20]. Then, Ref. [21] applies an online distributed Gaussian process method to scalar field mapping. These methods avoid communicating observations on networks. However, these methods do not provide error bounds with centralized aggregation methods and do not consider the sparse computation, causing the bad $\mathcal{O}(N^3)$ computational costs. Ref. [22] provides a local online Gaussian process evaluation method to reduce computation and inter-robot communications by only computing and communicating partial observations. Ref. [23] employs the SVGPR for multi-robot systems, in which each robot obtains the sparse subsets based on its local observations. Unfortunately, these approaches have bad global accuracy because the online evaluations only use local information.

B. Main Contributions

This letter proposes a distributed sparse online Gaussian process regression method for cooperative online scalar field mapping. The main contributions of this letter are as follows.

- Propose a distributed recursive Gaussian process based on dynamic average consensus for streaming data and cooperative online mapping. The error bounds between distributed consensus results and the centralized PoE results are guaranteed theoretically (Theorem 1).
- Propose a novel distributed online evaluation method for Gaussian process. Each robot online evaluates observations based on distributed consensus results instead of only local information to obtain better global accuracy without additional communications.
- Develop a resource-efficient cooperative online scalar field mapping method via distributed sparse Gaussian process regression. The performances of the proposed algorithms are evaluated by real online light field mapping experiments.

II. PRELIMINARIES AND SYSTEM MODELING

A. Problem Statement

(Network Model) Consider a team of p robots, labeled by $i \in V = \{1, \dots, p\}$. The communication networks at time t can be represented by a directed graph $\mathcal{G}(t) = (V, E(t))$ with an edge set $E(t) \subset V \times V$. We consider that $(i, j) \in E(t)$ if and only if node i communicates to node j at time t . Define the set of the neighbors of robot i at time t as $\mathbb{N}_{i,t} = \{j \in V \mid (i, j) \in E(t)\}$. The matrix $A(t) := [a_{ij,t}]_{i,j=1}^{p,p} \in \mathbb{R}^{p \times p}$ represents the adjacency matrix of $\mathcal{G}(t)$ where $a_{ij,t} \neq 0$ if $(i, j) \in E(t)$.

(Observation Model) Each robot i independently senses the fields $f : \mathcal{X} \rightarrow \mathcal{Y}$ and gets the measurements $y_{i,t} \in \mathcal{Y}$ with zero-mean Gaussian noise $e_{i,t}$ at time t , where $\mathcal{X} \subset \mathbb{R}^{n_x}$ is the input feature space for f and $\mathcal{Y} \subset \mathbb{R}$ is the corresponding output space. The observation model is given by

$$y_{i,t} = f(\mathbf{x}_{i,t}) + e_{i,t}, \quad e_{i,t} \sim \mathcal{N}(0, \sigma_e^2),$$

where $\mathbf{x}_{i,t} \in \mathcal{X}$ is the position of robot i at time t . Let the local datasets of robot i at time t be in the form $\mathbf{D}_{i,t} := \{\mathbf{X}_{i,t}, \mathbf{Y}_{i,t}\}$, where $\mathbf{X}_{i,t} = \{\mathbf{x}_{i,k}\}_{k=1}^t$, $\mathbf{Y}_{i,t} = \{y_{i,k}\}_{k=1}^t$ are the sets of observations from begin to current time t .

(Problem Description) In cooperative online field mapping mission, a team of robots explores the unknown fields f and gets the observation datasets $\mathbf{D}_{i,t}$. Then, each robot uses the datasets to online construct an estimation of the field $f_{i,t}$ and share information across the networks $\mathcal{G}(t)$. Finally, the mapping results of each robot achieves consensus and converges to the fields, i.e., $f_{i,t} \rightarrow f, \forall i \in V$ as $t \rightarrow \infty$.

B. Gaussian Process Regression

Let the unknown fields $f : \mathcal{X} \rightarrow \mathcal{Y}$ be the target regression functions. A robot can use Gaussian process regression [24] to predict the latent function value $f(\mathbf{x}^*)$ at the test data points $\mathbf{x}^* \in \mathcal{X}$ using the training datasets $\mathbf{D} = \{\mathbf{X}, \mathbf{Y}\}$ under the assumption that f follows a Gaussian process.

In GPR, the Gram function $K(\mathbf{X}, \mathbf{X}) := [\kappa(\mathbf{x}_i, \mathbf{x}_j)]_{i,j=1}^{N,N} \in \mathbb{R}$ is constructed from the kernel function $\kappa : \mathcal{X} \times \mathcal{X} \rightarrow \mathbb{R}$ which is defined over the product set of the feature space. We employ the squared exponential (SE) kernel given as

$$\kappa(\mathbf{x}_i, \mathbf{x}_j) = \sigma_f^2 \exp\left(-\frac{\|\mathbf{x}_i - \mathbf{x}_j\|^2}{\Sigma_\eta^2}\right) \quad (1)$$

with hyper-parameters $\{\sigma_f, \Sigma_\eta\}$. Then, the posterior distribution is derived as $\rho(\mathbf{x}^*) := \mathcal{P}(f(\mathbf{x}^*)|\mathbf{X}, \mathbf{Y}, \mathbf{x}^*) \sim \mathcal{N}(\mu(\mathbf{x}^*), \Sigma(\mathbf{x}^*))$, where

$$\begin{aligned} \mu(\mathbf{x}^*) &= K(\mathbf{x}^*, \mathbf{X})[K(\mathbf{X}, \mathbf{X}) + \sigma_e^2 \mathbf{I}]^{-1} \mathbf{Y}, \\ \Sigma(\mathbf{x}^*) &= K(\mathbf{x}^*, \mathbf{x}^*) \\ &\quad - K(\mathbf{x}^*, \mathbf{X})[K(\mathbf{X}, \mathbf{X}) + \sigma_e^2 \mathbf{I}]^{-1} K(\mathbf{X}, \mathbf{x}^*). \end{aligned} \quad (2)$$

In this letter, we assume the hyper-parameters can be typically selected by maximizing the marginal log-likelihood offline [24] and focus on GP predictions (2) for field mapping, like Refs. [18], [19], [21], [22] and [23].

C. Recursive Gaussian process update for streaming data

In the online mapping mission, the data arrives sequentially. At any time t , the new data point $\{\mathbf{x}_t, y_t\}$ is added to datasets $\mathbf{D}_t = [\mathbf{D}_{t-1}; \mathbf{x}_t, y_t]$ in streaming set. In this case, the Gaussian process prediction (2) will suffer from catastrophic forgetting and slow updating. To speed up the online mapping, we employ the recursive Gaussian process update [15],

$$\begin{aligned} \mu(\mathbf{x}^*) &= K(\mathbf{x}^*, \mathbf{X}_t) \boldsymbol{\alpha}_t, \\ \Sigma(\mathbf{x}^*) &= K(\mathbf{x}^*, \mathbf{x}^*) + K(\mathbf{x}^*, \mathbf{X}_t) \mathbf{C}_t K(\mathbf{X}_t, \mathbf{x}^*), \end{aligned} \quad (3)$$

where $\boldsymbol{\alpha}_t \in \mathbb{R}^t$ and $\mathbf{C}_t \in \mathbb{R}^{t \times t}$ are recursive updated variables. Suppose a new data point $\{\mathbf{x}_{t+1}, y_{t+1}\}$ has been

collected, the recursive updates are designed as,

$$\begin{aligned}\boldsymbol{\alpha}_{t+1} &= \begin{bmatrix} \boldsymbol{\alpha}_t \\ 0 \end{bmatrix} + q_{t+1} \mathbf{s}_{t+1}, \\ \mathbf{C}_{t+1} &= \begin{bmatrix} \mathbf{C}_t & \mathbf{0}_t \\ \mathbf{0}_t^T & 0 \end{bmatrix} + r_{t+1} \mathbf{s}_{t+1} \mathbf{s}_{t+1}^T, \\ \mathbf{Q}_{t+1} &= \begin{bmatrix} \mathbf{Q}_t & \mathbf{0}_t \\ \mathbf{0}_t^T & 0 \end{bmatrix} + \gamma_{t+1} \mathbf{e}_{t+1} \mathbf{e}_{t+1}^T, \\ \mathbf{s}_{t+1} &= \begin{bmatrix} \mathbf{C}_t K(\mathbf{X}_t, \mathbf{x}_{t+1}) \\ 1 \end{bmatrix}, \quad \mathbf{e}_{t+1} = \begin{bmatrix} \mathbf{Q}_t K(\mathbf{X}_t, \mathbf{x}_{t+1}) \\ -1 \end{bmatrix}\end{aligned}\quad (4)$$

with the scalars q_{t+1} , r_{t+1} and γ_{t+1} given by

$$\begin{aligned}q_{t+1} &= \frac{y_{t+1} - K(\mathbf{x}_{t+1}, \mathbf{X}_t) \boldsymbol{\alpha}_t}{\sigma_e^2 + \kappa(\mathbf{x}_{t+1}, \mathbf{x}_{t+1}) + K(\mathbf{x}_{t+1}, \mathbf{X}_t) \mathbf{C}_t K(\mathbf{X}_t, \mathbf{x}_{t+1})}, \\ r_{t+1} &= \frac{-1}{\sigma_e^2 + \kappa(\mathbf{x}_{t+1}, \mathbf{x}_{t+1}) + K(\mathbf{x}_{t+1}, \mathbf{X}_t) \mathbf{C}_t K(\mathbf{X}_t, \mathbf{x}_{t+1})}, \\ \gamma_{t+1} &= \frac{1}{\kappa(\mathbf{x}_{t+1}, \mathbf{x}_{t+1}) - K(\mathbf{x}_{t+1}, \mathbf{X}_t) \mathbf{Q}_t K(\mathbf{X}_t, \mathbf{x}_{t+1})}.\end{aligned}\quad (5)$$

Upon comparison with (3), $1/\gamma_{t+1}$ can be interpreted as the recursive predictive variance of the new data point \mathbf{x}_{t+1} given the observations at \mathbf{D}_t without noise. This property and the variable \mathbf{Q} will be used in Section IV for sparse approximation.

III. CONSENSUS-BASED DISTRIBUTED GAUSSIAN PROCESS REGRESSION

In this section, we introduce the distributed Gaussian process regression methods for cooperative online field mapping. Each robot constructs individual field map and aggregates the global map in a distributed fashion using dynamic average consensus methods.

In contrast to existing consensus-based distributed Gaussian process methods [18], [19] and [21], this letter employs the PoE method to design the discrete-time dynamic average consensus. The theoretical error bounds between distributed consensus aggregation results and centralized PoE aggregation results are derived first time. Moreover, we employ the character of the recursive Gaussian process to loosen the bounded derivative assumption for easier parameter selections on real online mapping.

A. Consensus-based distributed Gaussian posterior update

At time t , each robot i first samples a new training pair $\{\mathbf{x}_{i,t}, y_{i,t}\}$ in the fields. Then, robots recursive update local Gaussian process posterior $\rho_{i,t}^{[L]}$ by (3) (4). With some abuse of notations, denote $\rho_{i,t}^{[L]}$ and $\rho_{i,t}^{[D]}$ as the local and distributed Gaussian posterior results of robot i at time t , respectively.

Next, we employ discrete-time dynamic average consensus methods [25] for distributed aggregation. The first-order iterative aggregation process can be written as

$$\begin{aligned}\xi_{i,t+1} &= \xi_{i,t} + \sum_{j \in \mathbb{N}_{i,t}} a_{ij,t} (\xi_{j,t} - \xi_{i,t}) + \Delta \mathbf{r}_{i,t}, \\ \xi_{i,0} &= \mathbf{r}_{i,0}, \quad \Delta \mathbf{r}_{i,0} = \mathbf{0},\end{aligned}\quad (6)$$

where $\xi_{i,t}$ denotes the local consensus state of robot i at time t and $\Delta \mathbf{r}_{i,t} = \mathbf{r}_{i,t} - \mathbf{r}_{i,t-1}$ is the reference input, which determines the converged consensus results. We employ the PoE method to design the local reference input. Then, the distributed Gaussian process update can be designed as

$$\mathbf{r}_{i,t} = \begin{bmatrix} \mu_{i,t}^{[L]} \cdot (\hat{\Sigma}_{i,t}^{[L]})^{-1} \\ (\hat{\Sigma}_{i,t}^{[L]})^{-1} \end{bmatrix}, \quad \begin{bmatrix} \mu_{i,t}^{[D]} \\ \Sigma_{i,t}^{[D]} \end{bmatrix} = \begin{bmatrix} \xi_{i,t+1}^{[1]} \cdot (\xi_{i,t+1}^{[2]})^{-1} \\ (\xi_{i,t+1}^{[2]})^{-1} \end{bmatrix}, \quad (7)$$

where $\xi_{i,t+1}^{[k]}$ denotes the k -th element of the local consensus state and $\hat{\Sigma}_{i,t}^{[L]} := \Sigma_{i,t}^{[L]} + \sigma_n^2$ is the local Gaussian posterior variance with the correction biases σ_n^2 for avoiding singularity. Due to the theoretical foundation of consensus algorithms, the distributed aggregation mean $\mu_{i,t}^{[D]}$ will converge to the centralized PoE results

$$\hat{\mu} = \sum_{i=1}^p \frac{(\hat{\Sigma}_{i,t}^{[L]})^{-1}}{\sum_i^p (\hat{\Sigma}_{i,t}^{[L]})^{-1}} \mu_{i,t}^{[L]}, \quad (8)$$

which will be discussed latter. In particular, robots are only required to communicate the local consensus state $\xi_{i,t}$ with constant size, instead of the online datasets $\mathbf{D}_{i,t}$ with growing size.

B. Error bounds derivation for distributed fusion

For the derivation of distributed aggregation error bounds, we introduce the following assumptions.

Assumption 1: (Periodical Strong Connectivity). There is some positive integer $B \geq 1$ such that, for all time instant $t \geq 1$, the directed graph $(V, E(t) \cup E(t+1) \cup \dots \cup E(t+B-1))$ is strongly connected.

Assumption 2: (Non-degeneracy and Doubly Stochastic). There exists a constant $\varphi > 0$ such that $a_{ii,t} = 1 - \sum_{j \in \mathbb{N}_{i,t}} a_{ij,t} \geq \varphi$, and $a_{ij,t}$ ($j \in \mathbb{N}_{i,t}$) satisfies $a_{ij,t} \in \{0\} \cup [\varphi, 1]$, $\forall t \geq 1$. And there hold that $\mathbf{1}^T A(t) = \mathbf{1}^T$ and $A(t)\mathbf{1} = \mathbf{1}$, $\forall t \geq 1$.

The Assumption 1 describes the periodical strong connectivity between robots and Assumption 2 defines the parameters selection of adjacency matrix, which are common for average consensus methods [25].

Assumption 3: (Bounded Observations). There exists time invariant constants \bar{y} and $\bar{\mu}$ such that all observations $y_{i,t}$ and local Gaussian process predictions $\mu_{i,t}^{[L]}(\mathbf{x}^*)$ satisfy $|y_{i,t}| \leq \bar{y}$, $|\mu_{i,t}^{[L]}(\mathbf{x}^*)| \leq \bar{\mu}$, $\forall t \geq 1$, $\forall i \in V$, $\forall \mathbf{x}^* \in \mathcal{X}$.

The average consensus methods generally suppose the derivative of the consensus state is bounded [18], [19] and [25]. The derivative bounds are related to the consensus errors and can be used for parameter selections of the communication network in practice, like communication periods and adjacency matrix. However, the derivative is hard to get sometimes. This letter employs the character of the recursive Gaussian process to loosen this requirement to the bounded observations (Assumption 3) for easier parameter selections on online mapping. Moreover, since the Gaussian process predictions are determined by the observations and the prior kernel function, it is bounded as the observations.

Theorem 1: Suppose Assumptions 1 ~ 3 hold and each robot i runs recursive Gaussian process (3) and first-order consensus algorithms (6). Let $\hat{\delta}_1$, $\hat{\delta}_2$ and η be positive constants, where

$$\begin{aligned}\hat{\delta}_1 &= \frac{\bar{y}\sigma_f^2(\sigma_n^2 + \sigma_f^2)}{\sigma_n^2(\sigma_e^2 + \sigma_f^2)} + \frac{\bar{\mu}\sigma_f^4}{\sigma_n^2(\sigma_e^2 + \sigma_f^2)}, \\ \hat{\delta}_2 &= \frac{\sigma_f^4}{\sigma_n^2(\sigma_e^2 + \sigma_f^2)}, \\ \eta &= \frac{4(pB - 1)}{\varphi^{0.5p(p+1)B-1}}.\end{aligned}\quad (9)$$

Select the correction term σ_n^2 to satisfy $\sigma_n^2 \geq \frac{\eta\sigma_f^4}{\sigma_e^2 + \sigma_f^2}$. Then, the error bounds between $\mu_{i,t}^{[D]}(\mathbf{x}^*)$ and PoE results $\tilde{\mu}(\mathbf{x}^*)$ (8) at any test point \mathbf{x}^* will converge to

$$\lim_{t \rightarrow \infty} \left| \mu_{i,t}^{[D]}(\mathbf{x}^*) - \tilde{\mu}(\mathbf{x}^*) \right| \leq \alpha + \beta \tilde{\mu}(\mathbf{x}^*), \quad \forall i \in V, \mathbf{x}^* \in \mathcal{X}, \quad (10)$$

where

$$\alpha = \frac{\eta\hat{\delta}_1}{1 + \eta\hat{\delta}_2}, \quad \beta = \left| \frac{\eta\hat{\delta}_2}{1 - \eta\hat{\delta}_2} \right|. \quad (11)$$

Furthermore, if there is a constant $h > 0$, $\Delta \mathbf{r}_{i,t+1} = \mathbf{0}$ for any time $t > h$ holds, the error bounds will converge to zero, i.e., $\mu_{i,t}^{[D]}(\mathbf{x}^*) \rightarrow \tilde{\mu}(\mathbf{x}^*)$, $\forall i \in V, \mathbf{x}^* \in \mathcal{X}$ as time $t \rightarrow \infty$.

Proof: The detailed proofs are in the Appendix. ■

IV. DISTRIBUTED SPARSE GAUSSIAN PROCESS APPROXIMATION

To speed up the GPR for online mapping, it is necessary to design Gaussian process sparse approximation methods. In this section, we employ an information-efficient subset with M points to summarize the entire N training points for Gaussian process predictions. A novel distributed metric is proposed for data evaluations such that predictions have better global performance without additional communication costs.

A. Distributed sparse metrics for recursive Gaussian process

For a robot i , the recursive variable scalar $q_{i,t+1}$ and $r_{i,t+1}$ (5) for can be interpreted as the variance-weighted prediction at point $\mathbf{x}_{i,t+1}$ using datasets $\mathbf{D}_{i,t}$. Ref. [22] use the sum of the changes in posterior mean at all current sample points $\{\mathbf{x}_{i,1}, \dots, \mathbf{x}_{i,t}\}$ to denote the score for the observation $\{\mathbf{x}_{i,t+1}, y_{i,t+1}\}$, which has been derived as

$$\epsilon_{i,t+1} = \left| \frac{\boldsymbol{\alpha}_{i,t+1}^{[t+1]}}{\text{diag}(\mathbf{Q}_{i,t+1})^{[t+1]}} \right|, \quad (12)$$

where $[t+1]$ denotes the $(t+1)$ -th item of the vectors and $\text{diag}(\cdot)$ denotes the diagonal vectors of the matrix. However, for a multi-robot system, each robot i has different datasets $\mathbf{D}_{i,t}$ and recursive Gaussian process variables $\boldsymbol{\alpha}_{i,t}$, $\mathbf{C}_{i,t}$. The score (12) can only evaluate the points based on local information, which causes repeated information and bad global performances. A 1-D toy example is shown in Fig. 2. Two robots sample the 1-D toy function and compress observations. Compression based on only local information tends

Algorithm 1 Cooperative Online Filed Mapping Algorithm for Robot i

Require: new data $\{\mathbf{x}_{i,t}, y_{i,t}\}$, data size budget M_i

- 1: **initialize** empty datasets $\mathbf{D}_{i,0} = \{\}$, initialized Gaussian distribution $\rho_{i,0}^{[D]} = \rho_{i,0}^{[L]} = \mathcal{N}(\mathbf{0}, \boldsymbol{\Sigma}_0)$
- 2: **for** $t = 1, 2, \dots$ **do**
- 3: /* Sensing and Local Update */
- 4: Sample independent training point $\{\mathbf{x}_{i,t}, y_{i,t}\}$
- 5: $\mathbf{D}_{i,t} = \{\mathbf{D}_{i,t-1}; (\mathbf{x}_{i,t}, y_{i,t})\}$, $\tilde{M}_i = \text{Size}(\mathbf{D}_{i,t})$
- 6: Update local Gaussian process predictions (3)
- 7: $\rho_{i,t}^{[L]} = \mathcal{P}(f(\mathbf{x}^*)|\mathbf{D}_{i,t}, \mathbf{x}^*) = \mathcal{N}(\mu_{i,t}^{[L]}, \boldsymbol{\Sigma}_{i,t}^{[L]})$
- 8: /* Communication and Achieving Consensus */
- 9: Receive $\xi_{j,t}$ from neighbors $j \in \mathbb{N}_{i,t}$
- 10: Compute local consensus state $\xi_{i,t+1}$ (6)
- 11: Update distributed Gaussian process predictions (7)
- 12: $\rho_{i,t}^{[D]} = \mathcal{N}(\mu_{i,t}^{[D]}, \boldsymbol{\Sigma}_{i,t}^{[D]})$
- 13: Send $\xi_{i,t+1}$ to neighbors $j \in \mathbb{N}_{i,t+1}$
- 14: /* Distributed Data Compress (Algorithm 2) */
- 15: **if** $\text{DataSize } \tilde{M}_i > M_i$ **then**
- 16: $\mathbf{D}_{i,t} = \text{Compress}(\mathbf{D}_{i,t}, \rho_{i,t}^{[D]})$
- 17: **end if**
- 18: **end for**

to retain repeated information in common areas because of the same local metrics.

In Section III, we have obtained the distributed aggregation results based on consensus methods. And then we employ the the distributed aggregation results $\rho_{i,t}^{[D]}$ to improve the compression performances.

Bhattacharyya-Riemannian distance is employed to evaluate the sample points using the distributed aggregation results. For two Gaussian distributions $\nu(\mathbf{x}) = \mathcal{N}(\mu_1, \boldsymbol{\Sigma}_1)$ and $\varphi(\mathbf{x}) = \mathcal{N}(\mu_2, \boldsymbol{\Sigma}_2)$ over feature space \mathcal{X} , Bhattacharyya-Riemannian distance is defined as

$$\begin{aligned}d_{\mathcal{BR}}(\nu, \varphi) &= d_{\mathcal{B}}(\nu, \varphi) + d_{\mathcal{R}}(\boldsymbol{\Sigma}_1, \boldsymbol{\Sigma}_2), \\ d_{\mathcal{B}}(\nu, \varphi) &= \sqrt{(\mu_1 - \mu_2)^T \bar{\boldsymbol{\Sigma}}^{-1} (\mu_1 - \mu_2)}, \\ d_{\mathcal{R}}(\boldsymbol{\Sigma}_1, \boldsymbol{\Sigma}_2) &= \sqrt{\sum_{j=1}^{n_{\lambda}} (\log \lambda_j)^2},\end{aligned}\quad (13)$$

where $\bar{\boldsymbol{\Sigma}} = \frac{1}{2}(\boldsymbol{\Sigma}_1 + \boldsymbol{\Sigma}_2)$, and $\{\lambda_1, \dots, \lambda_{n_{\lambda}}\}$ is the eigenvalues of $\boldsymbol{\Sigma}_2^{-1} \boldsymbol{\Sigma}_1$. This metric (13) modifies the Hellinger distance by employing Riemannian item $d_{\mathcal{R}}$, which is efficient for the Gaussian variance representation [27].

Denote $\mathbf{S}_{i,k} := \{\mathbf{x}_{i,k}, y_{i,k}\} \subset \mathbf{D}_{i,t}$ as the evaluated observation. We design a distributed sparse metrics as

$$\phi(\mathbf{S}_{i,k}) := k_{\phi} \Omega \left(-d_{\mathcal{BR}}(\rho_{i,t}^{[D]}, \tilde{\rho}_{i,t,k}^{[L]}) \right) + (1 - k_{\phi}) \Omega(\epsilon_{i,k}), \quad (14)$$

$$\tilde{\rho}_{i,t,k}^{[L]} := \mathcal{P}(f(\mathbf{x}^*)|\mathbf{D}_{i,t} \setminus \mathbf{S}_{i,k}, \mathbf{x}^*), \quad (15)$$

where $k_{\phi} \in (0, 1)$ is a constant weight for the local score and distributed score and $\Omega(\cdot)$ is the normalization function for all evaluated observations. This letter uses the simple

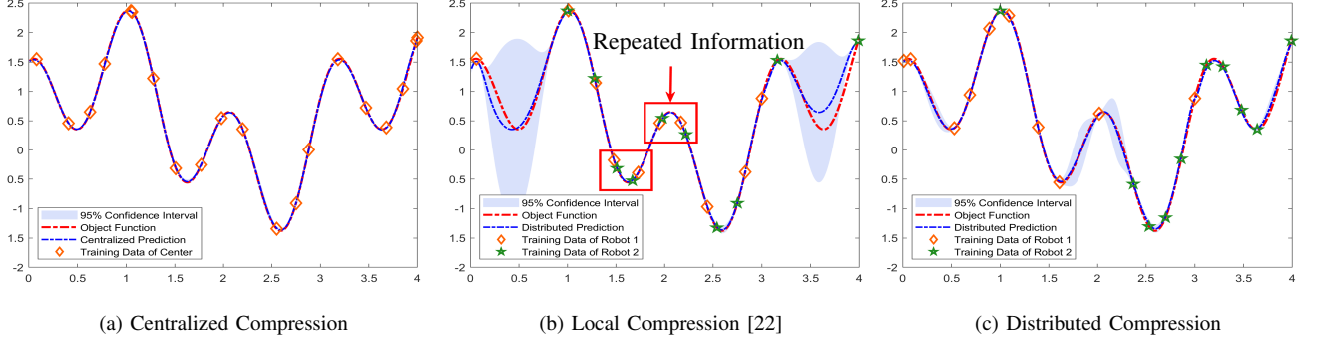


Fig. 2: A 1-D toy example with different compression methods. There are 2 robots sampling and predicting the objective function, respectively, where Robot 1 samples points ($N = 300$) from $x_{1,0} = 3$ to $x_{1,300} = 0$ and Robot 2 samples from $x_{2,0} = 1$ to $x_{2,300} = 4$. The shaded area represents 95% of the distributed GP confidence intervals. The diamond and star represent the sparse training data ($M = 10$) after the online compression. The toy objective function is $f(x) = \sin(2x) + \cos(6x) + 0.5$. (a) The centralized compression requires all real-time sample data. (b) Each robot compresses sample data locally, causing information repeated and globally inefficient. (c) Each robot compresses sample data based on distributed predictions with better performance.

min-max normalization. $\epsilon_{i,k}$ denotes the local score (12) for robot i about the evaluated observation $\mathbf{S}_{i,k}$. $\tilde{\rho}_{i,t,k}^{[L]}$ is the local recursive Gaussian process distribution removing the evaluated observation, which will be introduced latter.

In Section III, we have proved the distributed mean will converge to the centralized PoE results. Therefore, the distributed sparse metrics (14) can find observations of sufficient global utility. Moreover, when the distributed predictions have not converged or sample data size is small, the $\rho_{i,t}^{[D]}$ is similar to local predictions $\rho_{i,t}^{[L]}$ such that the distributed item in (14) is small and the local item can ensure sparse performance in this case.

B. Distributed sparse Gaussian process update

Then, we employ the distributed sparse metrics (14) to select the information-efficient subsets with M points and design the distributed sparse Gaussian process.

Reorder the elements of $\alpha_{i,t}$, $\mathbf{C}_{i,t}$, $\mathbf{Q}_{i,t}$ so that they are consistent with $\mathbf{S}_{i,k}$ being the last element in the current datasets $\mathbf{D}_{i,t}$, and define

$$\begin{aligned} \tilde{\alpha}_{i,k} &= \begin{bmatrix} \alpha_{i,t}^{[\tilde{k}]} \\ \alpha_{i,t}^{[k]} \end{bmatrix} = \begin{bmatrix} \tilde{\alpha}_{i,k}^{[1:M]} \\ \alpha_{i,k}^* \end{bmatrix}, \\ \tilde{\mathbf{C}}_{i,k} &= \begin{bmatrix} \mathbf{C}_{i,t}^{[k,\tilde{k}]} & \mathbf{C}_{i,t}^{[\tilde{k},k]} \\ \mathbf{C}_{i,t}^{[\tilde{k},k]} & \mathbf{C}_{i,t}^{[k,k]} \end{bmatrix} = \begin{bmatrix} \tilde{\mathbf{C}}_{i,k}^{[1:M,1:M]} & \mathbf{c}_{i,k} \\ \mathbf{c}_{i,k}^T & c_{i,k}^* \end{bmatrix}, \\ \tilde{\mathbf{Q}}_{i,k} &= \begin{bmatrix} \mathbf{Q}_{i,t}^{[\tilde{k},\tilde{k}]} & \mathbf{Q}_{i,t}^{[\tilde{k},k]} \\ \mathbf{Q}_{i,t}^{[k,\tilde{k}]} & \mathbf{Q}_{i,t}^{[k,k]} \end{bmatrix} = \begin{bmatrix} \tilde{\mathbf{Q}}_{i,k}^{[1:M,1:M]} & \mathbf{q}_{i,k} \\ \mathbf{q}_{i,k}^T & q_{i,k}^* \end{bmatrix}, \end{aligned} \quad (16)$$

where $\mathbf{C}^{[i,j]}$ denotes the elements of the matrix \mathbf{C} at i -th row and j -th column and $\tilde{k} = [1, \dots, k-1, k+1, \dots, M+1]$ denotes an index vector from 1 to $M+1$ expect k . Then, the recursive variables removing points $\mathbf{S}_{i,k}$ can be computed as

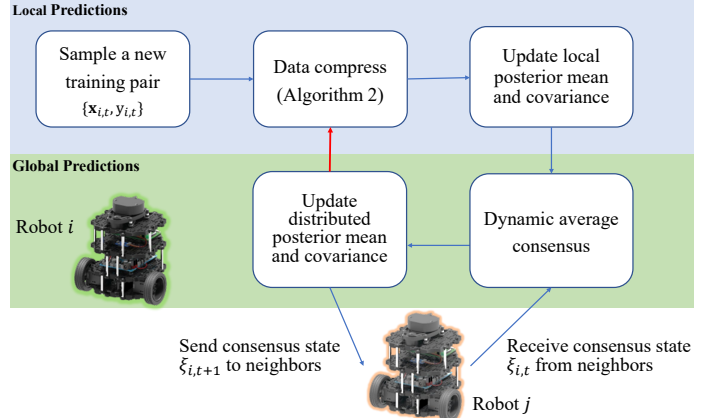


Fig. 3: Block diagram of the proposed Algorithm 1.

[15]

$$\begin{aligned} \hat{\alpha}_{i,k} &= \tilde{\alpha}_{i,k}^{[1:M]} - \frac{\alpha_{i,k}^*}{q_{i,k}^*} \mathbf{q}_{i,k}, \\ \hat{\mathbf{C}}_{i,k} &= \tilde{\mathbf{C}}_{i,k}^{[1:M,1:M]} + \frac{c_{i,k}^*}{(q_{i,k}^*)^2} \mathbf{q}_{i,k} \mathbf{q}_{i,k}^T - \frac{1}{q_{i,k}^*} \mathbf{\Gamma}_{i,k}, \\ \hat{\mathbf{Q}}_{i,k} &= \tilde{\mathbf{Q}}_{i,k}^{[1:M,1:M]} - \frac{1}{q_{i,k}^*} \mathbf{q}_{i,k} \mathbf{q}_{i,k}^T, \end{aligned} \quad (17)$$

where $\mathbf{\Gamma}_{i,k} = \mathbf{q}_{i,k} \mathbf{c}_{i,k}^T + \mathbf{c}_{i,k} \mathbf{q}_{i,k}^T$, so as to compute $\tilde{\rho}_{i,t,k}^{[L]}$ using the reduced $\hat{\alpha}_{i,k}$, $\hat{\mathbf{C}}_{i,k}$, $\hat{\mathbf{Q}}_{i,k}$ by (3).

C. Resource-efficient cooperative online mapping algorithm and complexity analysis

The entire cooperative online field mapping method is shown in Algorithm 1 and the block diagram is presented in Fig. 3. At time t , each robots samples at the field and updates local Gaussian process predictions $\rho_{i,t}^{[L]}$ by (3). Next, robots share local consensus state $\xi_{i,t}$ (6) with neighbors and update distributed Gaussian process predictions $\rho_{i,t}^{[D]}$ by

Algorithm 2 Distributed Data Compress for Robot i

Require: current datasets $\mathbf{D}_{i,t}$, distributed Gaussian process predictions $\rho_{i,t}^{[D]}$, data size budget M_i , local recursive variables $\alpha_{i,t}$, $\mathbf{C}_{i,t}$, $\mathbf{Q}_{i,t}$

- 1: **for** $k = 1, \dots, M_i + 1$ **do**
- 2: Compute test Gaussian posterior $\tilde{\rho}_{i,t,k}^{[L]}$ (15) without point $\mathbf{S}_{i,k} = \{\mathbf{x}_{i,k}, y_{i,k}\}$
- 3: Obtain distributed sparse metrics $\phi(\mathbf{S}_{i,k})$ (14)
- 4: **end for**
- 5: Find minimal information sample index
 $k^* = \operatorname{argmin}_{k \in \mathbf{D}_{i,t}} \phi_k^*$
- 6: Remove points $\{\mathbf{x}_{i,k^*}, y_{i,k^*}\}$ from datasets
 $\mathbf{D}_{i,t} = \mathbf{D}_{i,t} \setminus \{\mathbf{x}_{i,k^*}, y_{i,k^*}\}$
- 7: Update recursive variables with M dimensions (17)
 $\alpha_{i,t} = \hat{\alpha}_{i,k^*}, \mathbf{C}_{i,t} = \hat{\mathbf{C}}_{i,k^*}, \mathbf{Q}_{i,t} = \hat{\mathbf{Q}}_{i,k^*}$
- 8: **return** $\mathbf{D}_{i,t}, \alpha_{i,t}, \mathbf{C}_{i,t}, \mathbf{Q}_{i,t}$

(7). Moreover, robots use the distributed sparse metrics (14) to greedily select the information-efficient subsets (Algorithm 2). The recursive variables $\alpha_{i,t}$, $\mathbf{C}_{i,t}$, $\mathbf{Q}_{i,t}$ keep lower M dimensions by (17) for fast Gaussian process predictions.

A comparison of time and space complexity is presented in Table I. Recall that the robot number is p , each robot samples N training points and select M sparse points. For each robot, the recursive sparse update of local mapping yields $\mathcal{O}(N(M^2 + M^3))$ time complexity, which is significantly less than the time complexity of distributed recursive GP $\mathcal{O}(N^3)$. Compared to local data compression methods [22], [23], the proposed distributed sparse metrics have better global accuracy with additional $\mathcal{O}(NM^3)$ computation. Since $M \ll N$, the additional computation is acceptable for online mapping. Further comparisons are shown in experiments (Section V.B).

V. EXPERIMENTAL RESULTS

In this section, the proposed algorithm is validated by experiments with multiple TurtleBot3-Burger robots. Each robot shown in Fig. 1 is equipped with the BH1750FVI light sensor, sampling and mapping the light field online in a $7.5 \text{ m} \times 5 \text{ m}$ workspace. The locations of robots are obtained by April-Tags. The entire system is implemented in Robot Operating System (ROS).

In this experiment, there are 5 robots performing an exploration to map the light field in the workspace. The communication network is dynamic and determined by the distance between robots. The communication range between robots is set as 3 m and the corresponding adjacency matrix of networks is $a_{ij,t} = 0.1$ ($j \in \mathbb{N}_{i,t}$), $a_{ii,t} = 1 - \sum_{j \in \mathbb{N}_{i,t}} a_{ij,t}$. This letter does not consider path planning and the sample paths of robots are set as a fixed prior. Gaussian process hyper-parameters are set $\sigma_f^2 = 1$, $\Sigma_\eta = [26 \ 0; 0 \ 40]$. Observation noises and correction biases are set $\sigma_e^2 = \sigma_n^2 = 0.1$. The distributed weight is set $k_\phi = 0.2$. All 5 robots sample a total of $N = 1056 \times 5$ training points.

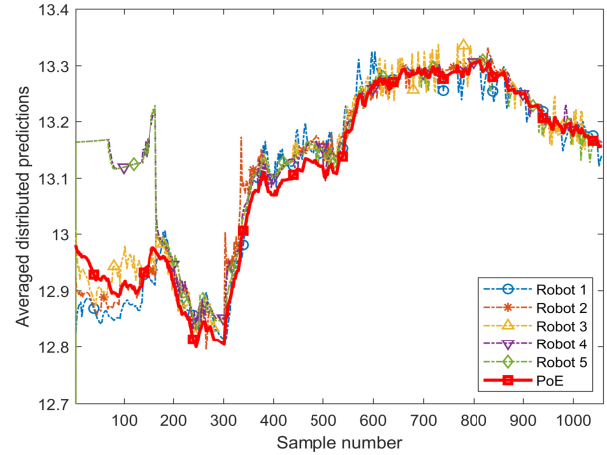


Fig. 4: The averaged distributed predictions and centralized PoE results for all test points.

A. Convergence validation of distributed aggregation

Select a 50×50 mesh grid in the workspace as the test points to construct the light field mapping. The size of sparse training subsets is set as $M = 13 \times 5$. The averaged distributed predictions of all 5 robots for all test points in the experiment and the centralized PoE results are shown in Fig. 4. The communication network is dynamic and Robots 4 and 5 are out of communication ranges of Robots 1, 2 and 3 at first time. When sample number $n > 166$, Robots 4 and 5 begin sharing information in the communication network and the distributed aggregation results of all robots converge to the centralized PoE results.

Fig. 5 represents the progress of this experiment and the corresponding distributed GP results of Robot 3 during time $t = 34$ ($n = 1056$) seconds. Fig. 5(a) shows the experiment snapshots and the robot number. Fig. 5(b) shows the results of the distributed online GP variance predictions for Robot 3 with the exploration trajectories of all robots. The black points denote the sparse subsets for GP predictions. Fig. 5(c) shows that the GP mean predictions for Robot 3 gradually converges to the real light field in Fig. 5(a). Compared to the local GP results of Robot 3 shown in Fig. 6, the distributed aggregation methods efficiently construct light field maps for unvisited areas.

B. Sparse prediction accuracy validation

To analyze the map accuracy with different GP prediction methods, 10×10 equal interval points in the workspace are sampled by hand as the test points. Fig. 7(a) shows the mean RMSE of the distributed predictions on the test points for all robots. Compared to the local data compression [22], the proposed distributed compression improves the prediction accuracy. Fig. 7(b) shows the mean online prediction computational time for all robots on 20 repeated experiments. The proposed sparse GP has an efficient constant prediction time with the growing sample datasets and the additional constant computational time for distributed metrics is acceptable on online mapping.

TABLE I: Computational Complexity for N streaming data.

Complexity	Full GPR [24]	Recursive GPR [15]	Distributed GPR [18], [19]	Distributed recursive GPR [21]	Local sparse GPR [22], [23]	This letter
Time	$\mathcal{O}(p^4 N^4)$	$\mathcal{O}(p^3 N^3)$	$\mathcal{O}(pN^4)$	$\mathcal{O}(pN^3)$	$\mathcal{O}(pNM^2)$	$\mathcal{O}(pN(M^2 + M^3))$
Space	$\mathcal{O}(p^2 N^2)$	$\mathcal{O}(p^2 N^2)$	$\mathcal{O}(pN^2)$	$\mathcal{O}(pN^2)$	$\mathcal{O}(pM^2)$	$\mathcal{O}(pM^2)$

*Compared to [22], [23], our method has better global accuracy with additional $\mathcal{O}(NM^3)$ computation, which is acceptable since $M \ll N$.

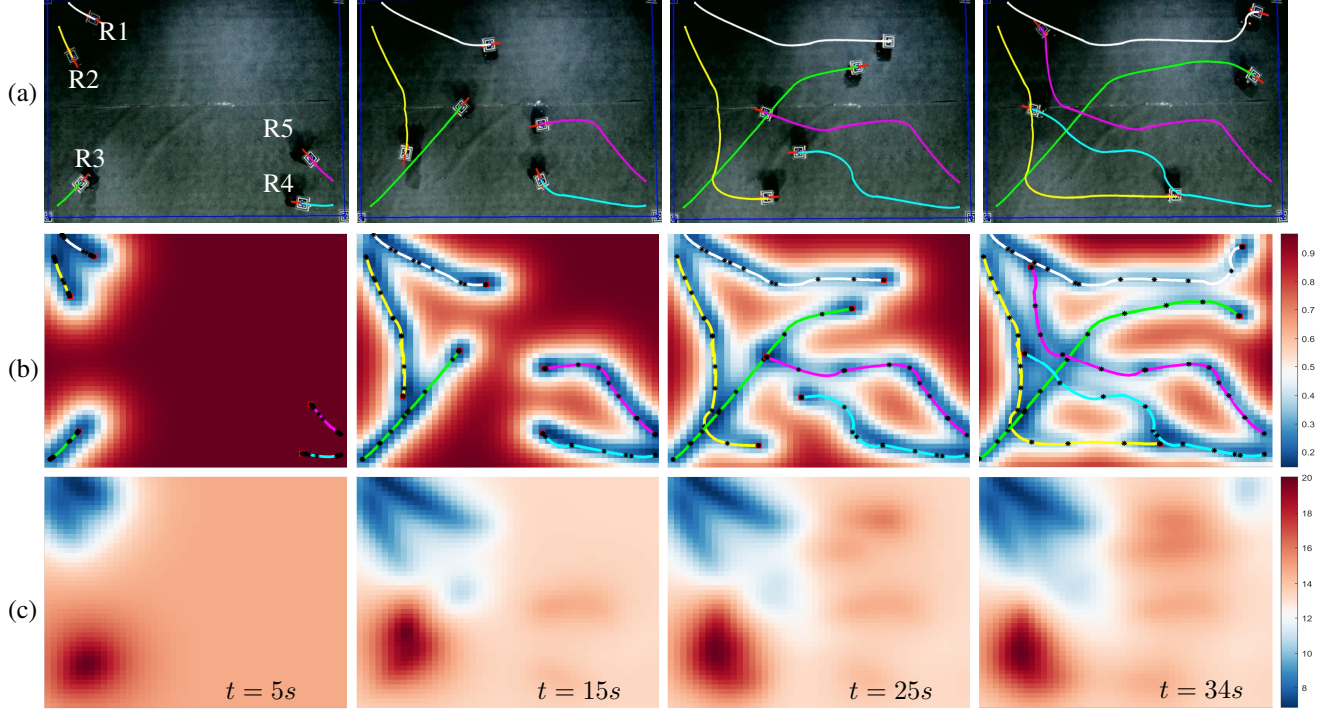


Fig. 5: A team of 5 robots cooperatively construct the online map of the light fields. (a) Experiment snapshots and the robot number. (b) Distributed online GP variance predictions for Robot 3 and the exploration trajectories of all robots. The black points denote the sparse subsets for GP predictions. (c) Distributed online GP mean predictions for Robot 3, which gradually converges to the real light field in (a).

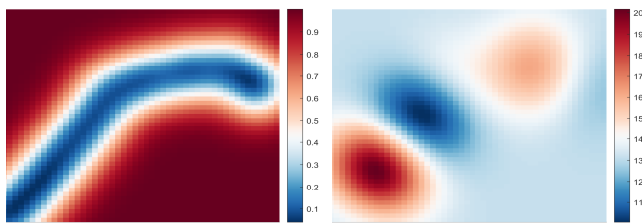


Fig. 6: Local Gaussian process mapping results of Robot 3. Compared to Fig. 5, the distributed aggregation methods efficiently construct light field maps for unvisited areas.

VI. CONCLUSIONS

This letter proposes a resource-efficient cooperative online field mapping method via distributed sparse Gaussian process regression. Novel distributed online sparse metrics are

developed such that robots can cooperatively evaluate observations with better global accuracy. The bounded errors of distributed aggregation results are guaranteed theoretically, and performances of proposed algorithms are validated by online light field mapping experiments. Our future work will focus on the distributed sparse GP hyper-parameters training and variance-based sample path planning.

APPENDIX: PROOF OF THEOREM 1

Without loss of generality, we consider the test data \mathbf{x}^* is a point here such that $\mu(\mathbf{x}^*) \in \mathbb{R}$, $\Sigma(\mathbf{x}^*) \in \mathbb{R}$. For the simplicity, we omit the test points (\mathbf{x}^*) in the following Gaussian process descriptions. We first derive the bounds of the reference input $\|\Delta \mathbf{r}_{i,t}\|$ in (6).

$$\Delta \mathbf{r}_{i,t+1} = \begin{bmatrix} \Delta \mathbf{r}_{i,t+1}^{[1]} \\ \Delta \mathbf{r}_{i,t+1}^{[2]} \end{bmatrix} = \begin{bmatrix} \mu_{i,t+1}^{[L]} \cdot (\hat{\Sigma}_{i,t+1}^{[L]})^{-1} - \mu_{i,t}^{[L]} \cdot (\hat{\Sigma}_{i,t}^{[L]})^{-1} \\ (\hat{\Sigma}_{i,t+1}^{[L]})^{-1} - (\hat{\Sigma}_{i,t}^{[L]})^{-1} \end{bmatrix}. \quad (18)$$

According to Ref. [24] and the SE kernel (1), the local Gaussian posterior variances have the bounds $0 < \Sigma_{i,t} \leq \sigma_f^2$.

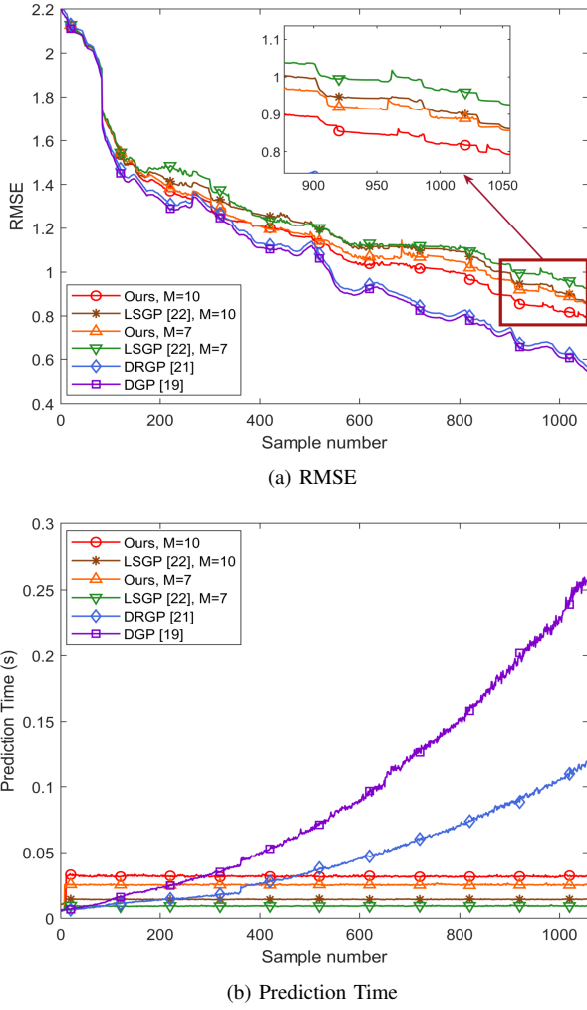


Fig. 7: Performance of the distributed GP [19], the distributed recursive GP [21], the local sparse GP [22] and the proposed Algorithm 1 in this experiment. The proposed algorithm has an efficient constant prediction time with better global accuracy.

Therefore, we derive

$$\sigma_n^2 \leq \hat{\Sigma}_{i,t+1}^{[L]} < \sigma_n^2 + \sigma_f^2, \quad (19)$$

Denote $K_*(\mathbf{x}_{t+1}) := K(\mathbf{x}^*, \mathbf{x}_{t+1})$ and $K_t(\mathbf{x}_{t+1}) := K(\mathbf{X}_t, \mathbf{x}_{t+1})$. The recursive updates of $\boldsymbol{\alpha}_{t+1}$ and \mathbf{C}_{t+1} (4) can be rewritten as

$$\begin{aligned} \boldsymbol{\alpha}_{t+1} &= \begin{bmatrix} \boldsymbol{\alpha}_t + q_{t+1} \mathbf{C}_t K_t(\mathbf{x}_{t+1}) \\ q_{t+1} \end{bmatrix}, \\ \mathbf{C}_{t+1} &= \begin{bmatrix} \mathbf{C}_t + r_{t+1} \mathbf{C}_t K_t(\mathbf{x}_{t+1}) K_t^T(\mathbf{x}_{t+1}) \mathbf{C}_t^T & r_{t+1} \mathbf{C}_t K_t(\mathbf{x}_{t+1}) \\ r_{t+1} K_t^T(\mathbf{x}_{t+1}) \mathbf{C}_t^T & r_{t+1} \end{bmatrix}, \end{aligned} \quad (20)$$

The Gram function $K_*(\mathbf{X}_{t+1}) = [K_*(\mathbf{X}_t), K_*(\mathbf{x}_{t+1})]$. Then, according to (3), we obtain

$$\begin{aligned} \mu_{i,t+1}^{[L]} - \mu_{i,t}^{[L]} &= \\ [K_*(\mathbf{X}_t), K_*(\mathbf{x}_{t+1})] \begin{bmatrix} \boldsymbol{\alpha}_t + q_{t+1} \mathbf{C}_t K_t(\mathbf{x}_{t+1}) \\ q_{t+1} \end{bmatrix} - K_*(\mathbf{X}_t) \boldsymbol{\alpha}_t \\ &= q_{t+1} (K_*(\mathbf{X}_t) \mathbf{C}_t K_t(\mathbf{x}_{t+1}) + K_*(\mathbf{x}_{t+1})). \end{aligned} \quad (21)$$

Similarly,

$$\hat{\Sigma}_{i,t+1}^{[L]} - \hat{\Sigma}_{i,t}^{[L]} = r_{t+1} (K_*(\mathbf{X}_t) \mathbf{C}_t K_t(\mathbf{x}_{t+1}) + K_*(\mathbf{x}_{t+1}))^2. \quad (22)$$

Then, $\Delta \mathbf{r}_{i,t+1}^{[1]}$ (18) can be rewritten as

$$\begin{aligned} \Delta \mathbf{r}_{i,t+1}^{[1]} &= \frac{\mu_{i,t+1}^{[L]} \cdot \hat{\Sigma}_{i,t}^{[L]} - \mu_{i,t}^{[L]} \cdot \hat{\Sigma}_{i,t+1}^{[L]}}{\hat{\Sigma}_{i,t+1}^{[L]} \cdot \hat{\Sigma}_{i,t}^{[L]}} \\ &= \frac{(\mu_{i,t+1}^{[L]} - \mu_{i,t}^{[L]}) \cdot \hat{\Sigma}_{i,t}^{[L]} - \mu_{i,t}^{[L]} \cdot (\hat{\Sigma}_{i,t+1}^{[L]} - \hat{\Sigma}_{i,t}^{[L]})}{\hat{\Sigma}_{i,t+1}^{[L]} \cdot \hat{\Sigma}_{i,t}^{[L]}}. \end{aligned} \quad (23)$$

Since the only different point between time t and $t+1$ is the \mathbf{x}_{t+1} , we have

$$\begin{aligned} \max |\mu_{i,t+1} - \mu_{i,t}| &= \frac{\sigma_f^2}{\sigma_e^2 + \sigma_f^2} |y_{t+1}|, \\ \max |\Sigma_{i,t} - \Sigma_{i,t+1}| &= \frac{\sigma_f^4}{\sigma_e^2 + \sigma_f^2}. \end{aligned} \quad (24)$$

which is obtained when $\mathbf{x}_{t+1} = \mathbf{x}^*$ and $\|\mathbf{x}_k - \mathbf{x}^*\| \rightarrow \infty$, $k = 1, \dots, t$. Suppose that the Assumption 3 holds, we derive

$$|\Delta \mathbf{r}_{i,t+1}^{[1]}| \leq \frac{\bar{y} \sigma_f^2}{\sigma_n^2 (\sigma_e^2 + \sigma_f^2)} + \frac{\bar{\mu} \sigma_f^4}{\sigma_n^2 (\sigma_n^2 + \sigma_f^2) (\sigma_e^2 + \sigma_f^2)} = \delta_1. \quad (25)$$

Similarly, $\Delta \mathbf{r}_{i,t+1}^{[2]}$ is bounded as

$$\Delta \mathbf{r}_{i,t+1}^{[2]} = \frac{\hat{\Sigma}_{i,t}^{[L]} - \hat{\Sigma}_{i,t+1}^{[L]}}{\hat{\Sigma}_{i,t+1}^{[L]} \cdot \hat{\Sigma}_{i,t}^{[L]}} \leq \frac{\sigma_f^4}{\sigma_n^2 (\sigma_n^2 + \sigma_f^2) (\sigma_e^2 + \sigma_f^2)} = \delta_2. \quad (26)$$

Define δ_{ξ_1} , δ_{ξ_2} as the consensus errors, i.e.,

$$\xi_{i,t+1}^{[1]} = \frac{1}{p} \sum_{i=1}^p \mu_{i,t}^{[L]} \cdot (\hat{\Sigma}_{i,t}^{[L]})^{-1} + \delta_{\xi_1}, \quad (27)$$

$$\xi_{i,t+1}^{[2]} = \frac{1}{p} \sum_{i=1}^p (\hat{\Sigma}_{i,t}^{[L]})^{-1} + \delta_{\xi_2},$$

According to the convergence of the FODAC algorithms (*Theorem 3.1 in [25]*), suppose the Assumptions 1, 2 hold, the consensus error δ_{ξ_1} , δ_{ξ_2} is bounded as,

$$\begin{aligned} |\delta_{\xi_1}| &\leq \frac{4(pB-1)\delta_1}{\varphi^{0.5p(p+1)B-1}}, \\ |\delta_{\xi_2}| &\leq \frac{4(pB-1)\delta_2}{\varphi^{0.5p(p+1)B-1}} \end{aligned} \quad (28)$$

when time $t \rightarrow \infty$.

Denote $\eta = \frac{4(pB-1)}{\varphi^{0.5}p(p+1)^{B-1}}$, $\zeta_\mu = \frac{1}{p} \sum_{i=1}^p \mu_{i,t}^{[L]} \cdot (\hat{\Sigma}_{i,t}^{[L]})^{-1}$, $\zeta_\Sigma = \frac{1}{p} \sum_{i=1}^p (\hat{\Sigma}_{i,t}^{[L]})^{-1}$. Let $|\delta_{\xi_2}| \leq \eta \delta_2 \leq \frac{1}{\sigma_n^2 + \sigma_f^2} \leq \zeta_\Sigma$, i.e., the σ_n^2 satisfies $\sigma_n^2 \geq \frac{\eta \sigma_f^4}{\sigma_e^2 + \sigma_f^2}$ such that we have $\zeta_\Sigma + \delta_{\xi_2} > 0$ for avoiding singularity. The difference between distributed the aggregation mean $\mu_{i,t}^{[D]}$ and the PoE results (8) can be written as,

$$\begin{aligned} |\mu_{i,t}^{[D]} - \tilde{\mu}| &\leq \left| \frac{\zeta_\mu + \delta_{\xi_1}}{\zeta_\Sigma + \delta_{\xi_2}} - \frac{\zeta_\mu}{\zeta_\Sigma} \right| \leq \left| \frac{\zeta_\Sigma \delta_{\xi_1} - \zeta_\mu \delta_{\xi_2}}{\zeta_\Sigma (\zeta_\Sigma + \delta_{\xi_2})} \right| \\ &\leq \left| \frac{\delta_{\xi_1}}{\zeta_\Sigma + \delta_{\xi_2}} - \tilde{\mu} \left(1 - \frac{\zeta_\Sigma}{\zeta_\Sigma + \delta_{\xi_2}} \right) \right| \\ &\leq \frac{\eta \delta_1 (\sigma_n^2 + \sigma_f^2)}{1 + \eta \delta_2 (\sigma_n^2 + \sigma_f^2)} + \left| \frac{\eta \delta_2 (\sigma_n^2 + \sigma_f^2)}{1 - \eta \delta_2 (\sigma_n^2 + \sigma_f^2)} \right| \cdot \tilde{\mu} \end{aligned} \quad (29)$$

Furthermore, if there is a constant $h > 0$, $\Delta \mathbf{r}_{i,t+1} = \mathbf{0}$ for any time $t > h$ holds, according to the Corollary 3.1 in [25], δ_{ξ_1} and δ_{ξ_2} will converge to zero. Then, we have $\mu_{i,t}^{[D]}(\mathbf{x}^*) \rightarrow \tilde{\mu}(\mathbf{x}^*)$, $\forall i \in V$, $\mathbf{x}^* \in \mathcal{X}$ as time $t \rightarrow \infty$.

REFERENCES

- [1] A. A. R. Newaz, M. Alsayegh, T. Alam, and L. Bobadilla, “Decentralized Multi-Robot Information Gathering From Unknown Spatial Fields,” *IEEE Robotics and Automation Letters*, vol. 8, no. 5, pp. 3070–3077, May 2023.
- [2] B. Zhou, H. Xu, and S. Shen, “Racer: Rapid collaborative exploration with a decentralized multi-uav system,” *IEEE Transactions on Robotics*, vol. 39, no. 3, pp. 1816–1835, 2023.
- [3] Z. Zhang, J. Yu, J. Tang, Y. Xu, and Y. Wang, “Mr-topomap: Multi-robot exploration based on topological map in communication restricted environment,” *IEEE Robotics and Automation Letters*, vol. 7, no. 4, pp. 10 794–10 801, 2022.
- [4] S. Saeedi, M. Trentini, M. Seto, and H. Li, “Multiple-robot simultaneous localization and mapping: A review,” *Journal of Field Robotics*, vol. 33, no. 1, pp. 3–46, 2016.
- [5] Y. Yang, Y. Xiao, and T. Li, “A survey of autonomous underwater vehicle formation: Performance, formation control, and communication capability,” *IEEE Communications Surveys & Tutorials*, vol. 23, no. 2, pp. 815–841, 2021.
- [6] T. X. Lin, S. Al-Abri, S. Coogan, and F. Zhang, “A distributed scalar field mapping strategy for mobile robots,” in *2020 IEEE/RSJ International Conference on Intelligent Robots and Systems (IROS)*, 2020, pp. 11 581–11 586.
- [7] T. M. C. Sears and J. A. Marshall, “Mapping of spatiotemporal scalar fields by mobile robots using gaussian process regression,” in *2022 IEEE/RSJ International Conference on Intelligent Robots and Systems (IROS)*, 2022, pp. 6651–6656.
- [8] L. Jin, J. Rückin, S. H. Kiss, T. Vidal-Calleja, and M. Popović, “Adaptive-Resolution Field Mapping Using Gaussian Process Fusion With Integral Kernels,” *IEEE Robotics and Automation Letters*, vol. 7, no. 3, pp. 7471–7478, July 2022.
- [9] M. Titsias, “Variational learning of inducing variables in sparse gaussian processes,” in *Proceedings of the Twelfth International Conference on Artificial Intelligence and Statistics*, vol. 5, 16–18 Apr 2009, pp. 567–574.
- [10] D. Burt, C. E. Rasmussen, and M. V. D. Wilk, “Rates of Convergence for Sparse Variational Gaussian Process Regression,” in *Proceedings of the 36th International Conference on Machine Learning*, May 2019, pp. 862–871.
- [11] M. Deisenroth and J. W. Ng, “Distributed gaussian processes,” in *Proceedings of the 32nd International Conference on Machine Learning*, 07–09 Jul 2015, pp. 1481–1490.
- [12] H. Liu, J. Cai, Y. Wang, and Y. S. Ong, “Generalized robust Bayesian committee machine for large-scale Gaussian process regression,” in *Proceedings of the 35th International Conference on Machine Learning*, vol. 80, 10–15 Jul 2018, pp. 3131–3140.
- [13] T. N. Hoang, Q. M. Hoang, and B. K. H. Low, “A distributed variational inference framework for unifying parallel sparse gaussian process regression models,” in *Proceedings of The 33rd International Conference on Machine Learning*, vol. 48, 20–22 Jun 2016, pp. 382–391.
- [14] H. T. Nghia, H. Q. Minh, and L. B. K. Hsiang, “A unifying framework of anytime sparse gaussian process regression models with stochastic variational inference for big data,” in *Proceedings of the 32nd International Conference on Machine Learning*, vol. 37, Lille, France, 07–09 Jul 2015, pp. 569–578.
- [15] L. Csató and M. Opper, “Sparse On-Line Gaussian Processes,” *Neural Computation*, vol. 14, no. 3, pp. 641–668, Mar. 2002.
- [16] T. D. Bui, C. Nguyen, and R. E. Turner, “Streaming Sparse Gaussian Process Approximations,” in *Advances in Neural Information Processing Systems*, I. Guyon, U. V. Luxburg, S. Bengio, H. Wallach, R. Fergus, S. Vishwanathan, and R. Garnett, Eds., vol. 30. Curran Associates, Inc., 2017.
- [17] B. Wilcox and M. C. Yip, “SOLAR-GP: Sparse Online Locally Adaptive Regression Using Gaussian Processes for Bayesian Robot Model Learning and Control,” *IEEE Robotics and Automation Letters*, vol. 5, no. 2, pp. 2832–2839, Apr. 2020.
- [18] Z. Yuan and M. Zhu, “Communication-aware Distributed Gaussian Process Regression Algorithms for Real-time Machine Learning,” in *2020 American Control Conference (ACC)*. Denver, CO, USA: IEEE, July 2020, pp. 2197–2202.
- [19] A. Lederer, Z. Yang, J. Jiao, and S. Hirche, “Cooperative Control of Uncertain Multiagent Systems via Distributed Gaussian Processes,” *IEEE Transactions on Automatic Control*, vol. 68, no. 5, pp. 3091–3098, May 2023.
- [20] G. P. Kontoudis and D. J. Stilwell, “Decentralized nested gaussian processes for multi-robot systems,” in *2021 IEEE International Conference on Robotics and Automation (ICRA)*, 2021, pp. 8881–8887.
- [21] D. Jang, J. Yoo, C. Y. Son, D. Kim, and H. J. Kim, “Multi-Robot Active Sensing and Environmental Model Learning With Distributed Gaussian Process,” *IEEE Robotics and Automation Letters*, vol. 5, no. 4, pp. 5905–5912, Oct. 2020.
- [22] M. E. Kepler and D. J. Stilwell, “An Approach to Reduce Communication for Multi-agent Mapping Applications,” in *2020 IEEE/RSJ International Conference on Intelligent Robots and Systems (IROS)*. Las Vegas, NV, USA: IEEE, Oct. 2020, pp. 4814–4820.
- [23] E. Zobaeidi, A. Koppel, and N. Atanasov, “Dense Incremental Metric-Semantic Mapping for Multiagent Systems via Sparse Gaussian Process Regression,” *IEEE Transactions on Robotics*, vol. 38, no. 5, pp. 3133–3153, Oct. 2022.
- [24] C. E. Rasmussen and C. K. I. Williams, *Gaussian Processes for Machine Learning*. The MIT Press, 11 2005.
- [25] M. Zhu and S. Martínez, “Discrete-time dynamic average consensus,” *Automatica*, vol. 46, no. 2, pp. 322–329, Feb. 2010.
- [26] T. Ding, R. Zheng, S. Zhang, and M. Liu, “Resource-efficient cooperative online scalar field mapping via distributed sparse gaussian process regression,” *arXiv preprint, arXiv:2309.10311*, 2023.
- [27] K. T. Abou-Moustafa and F. P. Ferrie, “A Note on Metric Properties for Some Divergence Measures: The Gaussian Case,” in *Proceedings of the Asian Conference on Machine Learning*, Nov. 2012, pp. 1–15.